Research Square

Preprints are preliminary reports that have not undergone peer review.
They should not be considered conclusive, used to inform clinical practice,
or referenced by the media as validated information.

Enhancing Spectral Absorption of Organic Dye Sensitizers through $ZnSO_4$-Mediated Coordination and Protonation for DSSCs Applications

A. M. Shahrul
Universiti Teknologi MARA Cawangan Pulau Pinang
N. D.M. Sin
Universiti Teknologi MARA Cawangan Pulau Pinang
ZHC Soh
Universiti Teknologi MARA Cawangan Pulau Pinang
M. H. Mamat
Universiti Teknologi MARA (UiTM)
Mj. Jalil
Universiti Teknologi MARA Cawangan Pulau Pinang
WI Nawawi
Universiti Teknologi MARA (UiTM)
R. Radzali
Universiti Teknologi MARA Cawangan Pulau Pinang
A. Supriyanto
Universitas Sebelas Maret
R. Suryana
Universitas Sebelas Maret
M. H. Abdullah
hanapiah801@uitm.edu.my

Universiti Teknologi MARA Cawangan Pulau Pinang

Research Article

Keywords: Dual-functional, Cationic Resonance, Protonation, Coordination, Spectral Absorption, Dye Sensitized Solar Cells

Posted Date: June 29th, 2026

DOI: https://doi.org/10.21203/rs.3.rs-10027694/v1

License: This work is licensed under a Creative Commons Attribution 4.0 International License.
Read Full License

Additional Declarations: No competing interests reported.

Abstract

This research examines the spectral improvement of organic-based dye-sensitized solar cells (DSSCs) via the incorporation of $ZnSO_4$ dual-functional dye additive. In this context, Zn^{2+} ions binds and coordinates anthocyanin molecules to the TiO_2 nanoparticles through its functional groups and stabilizes the flavylium-Zn^{2+}-TiO_2 system. Meanwhile, SO_4^{2-} helps boost the cationic resonance through protonation of the dye solution which enhanced the spectral photoactive of the flavylium cation. Then, this consequently stabilizes cationic resonance structure, optimizes orbital conjugation and enhances spectral absorption of the treated flavylium dye molecules. The chemical, morphological and electrical properties of the $ZnSO_4$ treated samples were characterized through uv-vis spectroscopy (UV-Vis), Fourier-transform Infra-Red (FTIR), field emission scanning electron micrograph (FESEM), cyclic voltammetry (CV), incident photon-to-current efficiency (IPCE), and current–voltage (J–V) measurements. A limited photovoltaics performance was seen in the untreated DSSC (UTD cell), as revealed by the open-circuit voltage (V_{OC}) of 0.46 V, the short-circuit current density (J_{SC}) of 0.52 mA/cm2, the fill factor (FF) of 0.44, and the overall efficiency (η) of 0.11%. In contrast, the optimized 8-ZnTD cell achieved a significantly improved V_{OC} of 0.53 V, J_{SC} of 1.74 mA/cm², FF of 0.41, and η of 0.38%. These findings validate the dual functional mechanisms of $ZnSO_4$ (Zn^{2+} chelation/coordination and protonation through SO_4^{2-}) which act in tandem to stabilize the cationic resonance of the flavylium dye, extend conjugation and the enhance spectral integrity of the absorption spectra. This method becomes a synergistic approach to revert natural dye-based DSSCs, which lays the groundwork for future additive design in bio-inspired photovoltaics.

Introduction

Due to their low manufacturing costs, aesthetic versatility, and compatibility with both synthetic and organic sensitizers, a third-generation photovoltaic technology namely DSSCs have becoming as an alternative to the silicon-based solar cell. Among their potential sensitizers, anthocyanins is a type of natural dye that contains flavonoid pigments found in fruits and flowers have been used because of their natural metal-chelating properties, broad spectrum absorption, and environmental sustainability. However, the performance of DSSC with bare anthocyanin sensitizer are still lower owing to its weak anchoring to TiO_2 surfaces, and poor chemical stability [1], [2].

To address these limitations, scientists have investigated several strategies, such as modifying the interactions at the dye–semiconductor interface by adding metal ions. In this regard, it has been reported that the use of trivalent ions, like Al^{3+}, improves light harvesting and dye adsorption by binding more dye molecules to the TiO2 sites through supramolecular scaffolding, which leads to notable improvements in Jsc [3]. Furthermore, the redox activity and interfacial effects of divalent ions such as Cu^{2+} and Fe^{2+} have been reported to modulate the TiO_2 interfaces and the corresponding photovoltaic performances of DSSCs cell [4], [5]. Summing up, these studies demonstrated that the modification at

the semiconductor coordination focusing on the metal–dyes-TiO^2 is a promising technique for the enhancement of the organic sensitizer-based DSSCs.

But despite these developments, Zn^{2+}, another divalent, redox-inert ion with moderate Lewis's acidity has not received enough attention. According to some reports, adding Zn^{2+} to an anthocyanin solution is known to create stable bidentate complexes with the hydroxyl and carbonyl groups of the anthocyanin. This process has been reported to improve dye–TiO_2 anchoring and stabilized the flavylium tautomer cation [6]. In other studies, it was claimed that the anthocyanin molecules will undergo a controlled protonation process when treated with SO_4^{2-} anion in the dye sensitizer solution. Without causing an excessive protonation or dye degradation, the anthocyanin tautomer will be shifted in favour of the photoactive flavylium equilibrium by this process [7]. Thus, the combined and dual-functional behaviours that provide metal coordination through Zn^{2+} and its pH modulation capability through SO_4^{2-} clearly set $ZnSO_4$ apart from the earlier studies that either doped in single metal ions or used their common salts, like nitrates (NO_3^-) or chlorides (Cl^-). These methods frequently isolate the impact of each element, even though they interact and collaboratively work within the same system. In other words, focusing solely on the metal ion and ignoring the influence of counterion that could weaken or eradicate other components of the system could lead to improper observations and findings.

Furthermore, Cl^- and NO_3^- counterions often exhibits weaker acidifying effects in comparison to SO_4^{2-}. This situation prevents the establishment of the desired pH shift of the treated dye solution which destabilized its capacity to harvest light [8]. Additionally, $ZnCl_2$ and $Zn(NO_3)_2$ are highly soluble, which could lead to osmotic stress, ionic crowding, and deterioration of the dye adsorption layer [14]. Another drawback of both salts is due to the formation of soluble complexes such as $[ZnCl_4]^{2-}$ and $[Zn(NO_3)_4]^{2-}$ that decreases the accessibility of free Zn^{2+} ions for direct coordination with anthocyanin functional groups [9]. As a results of these reactions, the development of Ti–O–Zn bridges at the semiconductor interface and the formation of stable Zn^{2+}–dye chelates may be disrupted by the formation of these undesirable ligands. Moreover, another drawback of Cl^- ion is that it has adverse reactions when exposed to light to produce reactive species like Cl• radicals which can break down organic dyes and jeopardize the stability and stability of the organic dyes [11]. Similarly, the addition of NO_3^- ions might promote photoreduction, which would lead to the formation of parasitic electron channels and an increase in recombination losses [12].

However, in the case of $ZnSO_4$ additive, the dissolution process makes Zn^{2+} more labile, which enhances its ability to chelate with the dye's functional groups and subsequently promotes robust anchoring to TiO_2 surfaces [10]. In this case, $ZnSO_4$ functions as a chemically tuneable additive that combines coordination chemistry and solution-state modulation which preventing interface oversaturation and offering moderate solubility and ionic strength. Furthermore, SO_4^{2-}ions are thought to be electrochemically inert species that support redox stability and minimize adverse reactions [13]. This makes it possible to simultaneously improve dye stability and redox reversibility, which are difficult to obtain with metal ion doping alone.

To the best of our knowledge, $ZnSO_4$ has neither been used nor reported as a dual-functional chemical agent added to an anthocyanin dye sensitizer as reported in this study. The mechanistic role of $ZnSO_4$ as a dual-functional additive in anthocyanin-sensitized DSSCs which provides metal coordination through Zn^{2+} and its pH modulation capability through SO_4^2 is worth to be explored. These combined effects were characterized by FESEM, EDX, UV-Vis, FTIR, I-V and IPCE.

Experimental

The fabrication of porous TiO_2 photoelectrodes was carried out following the methodology established in our earlier work [15]. For the natural dye preparation, the complete anthocyanin extract derived from blackberry fruits was obtained as previously reported in [16]. The dye solution was then divided into five separate vials, each containing 10 mL. One vial served as the untreated control (UTD), while the remaining four were supplemented with $ZnSO_4$ (99.99%, Sigma Aldrich) at different concentrations: 0.2 g/10 mL (2-ZnTD), 0.6 g/10 mL (6-ZnTD), 0.8 g/10 mL (8-ZnTD), and 1.0 g/10 mL (10-ZnTD). The pH of each solution was determined using an E-Digital pH meter (model 8424).

Then after, all the photoelectrodes were simultaneously immersed in their respective dye solutions. The counter electrode layer was applied on ITO conducting side using HB pencil lead graphite (Faber Castell). The electrolyte mixture was made up of 0.05 M iodine (I_2, Sigma Aldrich), 0.5 M tetrabutylammonium iodide (TBAI, Sigma Aldrich), and 10 mL of acetonitrile. For the photovoltaics measurement, the photoelectrode and counter electrode were clamped together, the redox electrolyte was added to the cell by capillary action through the ITO layers that were sandwiched together.

FESEM, NOVA NANOSEM 450 with Energy Dispersive X-ray spectroscopy (EDX) was used to look at the surface morphology and elemental composition. FTIR (Thermo Scientific Nicolet 6700, OMNIC 8 software) is used to investigate the functional groups in the dye solutions and a UV-Vis spectrophotometer (Perkin Elmer Lambda 25) to record the optical absorption spectra.

Keithley 4200 SCS system is used to measure the current–voltage (I–V) characteristics of the dye-sensitized solar cells (DSSCs) under LED light. Next, Peccel PEC-S20 Action Spectrum Measurement System is used to measure IPCE spectra, which covered the 300–900 nm wavelength range while under DC bias. Autolab PGSTAT204 instrument is used to do CV on the samples to probe their electrochemical properties. The measurements were taken at a scan rate of 100 mV/s over a potential range of − 1.0 to + 1.0 V. The CV setup used three electrodes: platinum (Pt) as the counter electrode, glassy carbon as the working electrode, and Ag/AgCl as the reference electrode.

Result and Discussion

3.1 FESEM and EDX

FESEM in Fig. 1(a) and (b) shows that TiO_2 photoelectrodes that was immersed in $ZnSO_4$-treated anthocyanin (8-ZnTD), denoted as TiO_2/8-ZnTD, and those that was sensitized with unmodified anthocyanin (UTD), denoted as TiO_2/UTD. It is clearly observed that both images have distinctively showing variations in the surface morphology and shapes. The TiO_2/8-ZnTD sample has a surface that is inhomogeneous in term of sizes and shapes between rounded aggregates and native TiO_2 nanoparticles. The difference is probably attributed to the Zn^{2+}-anthocyanin complexes that were formed owing to chelation-induced stabilization and multilayered dye aggregation. Generally, Zn^{2+} ions interact directly with TiO_2 surfaces and then altering its structure arrangement as well as the grain boundaries, in which it elucidates the observed difference in the size. The mixed morphology characteristics seen in this study can be associated with better light scattering and more dye loading to the photoelectrode, as reported by Zhang et al. [17]. Their study demonstrates that the alteration of TiO_2 surfaces with Zn^{2+} improves dye-semiconductor coupling and refines interfacial architecture in DSSCs.

The surface morphology of the TiO_2/UTD photoelectrode, on the other hand, exhibits a more uniform and well-distributed nanoparticles distribution. The observed uniformity suggests an absence of Zn^{2+} coordination, as anthocyanin adheres via weaker physical interactions to TiO_2 nanoparticles, resulting in inconsistent coverage, less nanoparticles aggregations and limited structural reorganization. The absence of secondary aggregation within the film makes the interface simpler, however this could lead to instability and inefficient charge transport in the dye molecules. Similarly, Li et al. [18] reported that the adsorption of unmodified dye onto TiO_2 nanoparticles results in the formation of discontinuous and tiny cracks lines that might contributes to an elevated recombination sites and diminished photovoltaic efficiency.

The difference in the size and shape of the nanoparticles observed in the two samples indicates that Zn^{2+} works as both a chelating agent and a shape modulator. Zn^{2+} enhances the nanoscale architecture of the photoelectrode by facilitating dye aggregation and interfacial restructuring, which is crucial for optimizing electron injection, light harvesting, and the overall efficiency of DSSCs.

Figures 1 (c) and (d) show the EDX spectrum of both samples between TiO_2/8-ZnTD and TiO_2/UTD, respectively. The presence of distinct Zn peaks in TiO_2/8-ZnTD at 1.0 keV, 8.6 keV, and 9.6 keV proves the effective binding of zinc ions to the TiO_2 surface. This suggests that Zn^{2+} interacts through either surface complexation or partial lattice substitution, consistent with prior research on metal ion doping in semiconductor [19]. This is closely aligned with elemental analysis from previous investigations, indicating that Zn^{2+} plays a structural role in modifying the dye-TiO_2 interface. In other study, Devi et al. demonstrated the integration of Zn^{2+} into TiO_2 nanostructures led to enhanced dye adsorption and surface uniformity, thereby improving the overall interface quality of the dye-sensitized solar cell applications [20]. Simialrly, Pawar et al. reported that their SEM and EDX analysis showed that TiO_2/ZnO nanocomposites improved dye retention and reduced surface defects of the nanocomposite's film [21]. Again, Yildiz et al. [22] revealed that Zn^{2+}-modified TiO_2 nanotubes exhibited improved elemental homogeneity and reduced surface recombination sites of the film.

Furthermore, a study by Ghosh et al. [19] demonstrated that Zn^{2+} ions can occupy interstitial or substitutional sites in TiO_2 lattices, which improves the distribution of surface charge and facilitates the interaction between dye and semiconductor [23]. The sulfur peak at about 2.3 keV shows that sulfate ions from $ZnSO_4$ are also present. These observations indicated for the successful incorporation of $ZnSO_4$ in the TiO_2/8-ZnTD photoelectrode film. The results substantiate the interpretation that the integration of Zn^{2+} and SO_4^{2-}, corroborated by EDX, is not only compositional but also functionally relevant to interfacial engineering.

3.2 Chemical Reaction and pH Shift

Figure 2 shows the images of several dyes' solution with respect to different amount of $ZnSO_4$, and Table 1 tabulates the pH reading for the respective dye solutions. It can be witnessed that adding more $ZnSO_4$ makes the dye solution's red color stronger, which is closely related to the increases of dye's acidity which were extensively documented in pH-responsive anthocyanin research. For instance, Roy et al. [24] conducted a review on the ability of anthocyanins to change color under pH variations. They discovered that the red hues linked to flavylium are prevalent in acidic environment, while blue or purple hues connected with chalcone and hemiketal appear at higher pH levels. It was also highlighted that metal ions can influence this behavior by increasing the protonation state of the dye through metal-ligand coordination and the release of protons (H^+). Upon the dissolution process of $ZnSO_4$, Zn^{2+} ions are produced and subsequently chelate with the electron-donating groups such as hydroxyls and carbonyls of the anthocyanin backbone. The chelation process involves removing protons from ligands, which releases H^+ ions into the dye solution and raises its acidity levels. The increase in acidity causes anthocyanin molecules to change into their flavylium cation form, which causes the deepening red color seen in the sample series. The dissolution and proton removal reaction are as shown in Eqs. (1) and (2) below.

Step 1: The Zn^{2+} ion is a small and highly charged cation that exhibits a strong attraction to water molecules, leading to their hydrolysis.:

$$\mathrm{Zn^{2+} + H_2O \rightarrow \ [Zn(OH)]^{+} + H^{+}} \quad \text{Eq. 1}$$

Step 2: Further hydrolysis (under excessive concentrations or pH levels). At elevated Zn^{2+} concentrations or under pH conditions, additional hydrolysis may take place:

$$\mathrm{[Zn(OH)]^{+} + H_2O \rightarrow \ Zn(OH)_2 + H^{+}} \quad \text{Eq. 2}$$

Table 1
The pH reading for each of the ZnTD dye solutions in comparison to UTD

Sample	10-ZnTD	8-ZnTD	6-ZnTD	2-ZnTD	UTD
pH	2.61	2.82	3.16	3.52	3.76

In the same way, Rhim et al. [25] reported that anthocyanin-based indicators exhibit distinct colour changes when subjected to acidic conditions, thereby validating the dye's responsiveness to proton accumulation. Again, a study conducted by Khoo et al. [26] highlighting that the intensity and stability of anthocyanin colour are significantly affected by pH levels and the presence of metal ions, with Zn^{2+} contributing to enhanced red coloration through protonation and structural stabilization.

3.3 UV-Vis Spectroscopy, UV-Vis

Figure 3 presents the UV-Vis absorbance spectra of the UTD in comparison to all the ZnTD dye solutions. The spectra of all the Zn-treated anthocyanin (ZnTD) demonstrate an apparent rise in optical density and a slightly bathochromic shift in peak wavelength with rising Zn^{2+} concentration. The UTD generally displays a broad absorbance peak near 520 nm, which is associated with $\pi \rightarrow \pi^*$ transitions occurring within its conjugated flavylium structure. Following the incorporation of Zn^{2+}, there is a significant increase in peak intensity, accompanied by a slight shift in maximum absorbance toward approximately 540 nm. The slightly observed red shift indicates that Zn^{2+} coordination modestly broadens the conjugation system and reduces the HOMO–LUMO gap, which boosts visible light absorption, a key factor influencing the photocurrent [27]. It was reported that the coordination of Zn^{2+} ions with anthocyanin is established through the hydroxyl group on the A-ring and the carbonyl group on the C-ring, resulting in the formation of a stable bidentate complex. As a result of this coordination, the photostability, electronic transitions, molar absorptivity and spectral broadening of the dye molecules sensitizer were enhanced. These characteristics is consistent with the findings of Kong et al. [28], which demonstrated that metal–anthocyanin complexes exhibit enhanced light–matter interaction and superior charge transfer characteristics. Similarly, Gulcin et. al [29] indicate that metal ions such as Zn^{2+} exhibit a preference for binding to oxygen-rich sites that possess suitable geometry, with the strength of chelation being affected by the type of donor atom and its spatial orientation. Additionally, Adeagbo et. al. [30] noted that metal–anthocyanin complexes generally engage the C4 carbonyl and A-ring hydroxyls, resulting in the formation of stable chelates that improve spectral properties and dye–semiconductor interactions. The observable deepening of solution color, transitioning from pale red to deep crimson as shown in the inset of Fig. 3 provides additional evidence for the establishment of stable Zn–anthocyanin complexes characterized by increased chromophore density.

The heightened absorbance observed in the 520–550 nm range corresponds effectively with the solar spectrum, facilitating enhanced photon capture and an elevated photocurrent density J_{SC}. In DSSCs, the Zn^{2+}-treated anthocyanin demonstrates enhanced light absorption and improved anchoring to TiO_2 surfaces. This enhancement leads to improved electron injection efficiency and a reduction in recombination losses, which accounts for the observed increase in J_{SC}. The dual function of Zn^{2+}, first serving as both a spectral modulator and an interfacial stabilizer has renders it a significant additive for natural dye systems, particularly in contexts where photostability and spectral alignment frequently pose challenges. Hao et al. [31] reported that metal ion coordination can significantly enhance the photovoltaic performance of natural dyes by improving both light absorption and the interaction between the dye and semiconductor.

3.4 Fourier Transform Infra-red, FTIR

The FTIR spectra Fig. 4 (a) provide conclusive evidence of metal–ligand chelation predominantly involving the hydroxyl and carbonyl functional groups of the dye molecule. Such behavior is generally attributed to the free hydroxyl groups bond strongly with each other, especially with the general broad spectrum of the UD in the O–H stretching region (~ 3200–3600 cm^{-1}). However, after the treatment with Zn^{2+}, this band exhibits a reduction in width and a shift towards lower wavenumbers, suggesting the establishment of Zn^{2+} ions and hydroxyl oxygen atoms coordination domination. This coordination disrupts hydrogen bonding and reduces vibrational freedom, a hallmark of phenolic chelation. Mollaamin et al. [32] reported that this behaviour is closely associated with Zn^{2+} binding that leads to spectral narrowing and a red shift of the O–H band due to the depletion of electron density.

Additionally, the C = O stretching region (about 1650–1720 cm^{-1}) can also help confirm chelation. In the untreated anthocyanin, the carbonyl group on the C-ring is shown by a clear and sharp band. However, this absorbance profile moves down after the Zn^{2+} treatment which is due to the metal coordination takes electrons away from the carbonyl oxygen. This interaction, which is consistent with bidentate chelation involving both hydroxyl and carbonyl groups, weakens the C = O bond and changes its vibrational energy. Al-Saadi et al. [33] concluded that this similar characteristic is stems from the increased dye stability and stable metal–oxygen bonding in their aqueous anthocyanin–Zn complexes. After treatment with Zn^{2+}, the C–O–C fingerprint region (around 1000–1300 cm^{-1}) shows small changes and changes in intensity. The vibrations is also linked to ether and glycosidic linkages due to secondary effects of chelation. According to Custodio-Mendoza et al. [34], Zn^{2+} coordination can influence fingerprint vibrations by stabilizing the dye's π-system and reducing vibrational coupling between nearby functional groups. The observed spectral changes indicate that Zn^{2+} establishes a stable bidentate complex with anthocyanin in solution, primarily engaging the A-ring hydroxyl and C-ring carbonyl groups. The vibrational shifts observed in the O–H and C = O regions serve as direct evidence of chelation, whereas the fingerprint region indicates secondary structural effects. The observed spectral evolution with increasing Zn^{2+} concentrations (e.g., 2-ZnTD to 10-ZnTD) indicates a dose-dependent coordination model, wherein elevated Zn^{2+} levels result in more significant vibrational shifts and enhanced complex formation.

Figure 4(b) shows the FTIR spectra of 8-ZnTD/TiO_2 against UTD/TiO_2, which were performed to investigate the vibrational properties of Ti-O-Zn-dye molecules. It can be clearly noticed that the 1000–1700 cm^{-1} region provides clear evidence of Zn^{2+} and SO_4^{2-} coordination within the dye-Zn^{2+}–TiO_2 system. In particular, the 1200–1400 cm^{-1} range representing Zn^{2+} interaction with the anthocyanin's hydroxyl, OH and glycosidic moieties, reinforcing the dye's structural stability [35]. In addition, more intense differences can be observed in the 1500–1700 cm^{-1} region, where shifts in carbonyl and aromatic stretching vibrations indicate stronger dye–TiO_2 binding facilitated by Zn^{2+} cations [36] [37].

The accompanying schematic supports this interpretation, demonstrating Zn^{2+} as a molecular bridge connecting anthocyanin dye molecules to the TiO_2 surface as illustrated by the inset of the Fig. 4. The

dual coordination improves dye anchoring and interfacial stability which then contributed to effective charge transfer in dye-sensitized systems. The absence of similar characteristics in the UTD sample validates the importance of Zn^{2+}–TiO_2 interactions for dye's adsorption and coordination.

In this regard, solution-phase FTIR analysis identifies key chelation sites and coordination geometry, whereas TiO_2-immobilized FTIR analysis reveals interfacial stabilization and the behavior of dye anchoring. Combining these two analyses is essential for interpreting the dual role of Zn^{2+} in DSSC systems. Therefore, the incorporation of Zn^{2+} into dye solution modulates the electronic structure of the dye, meanwhile attaching them on TiO_2 explains the coupling affects between the dye and semiconductor as well as the efficiency of charge transfer.

3.5 Cyclic Voltammetry, CV

Figure 5 depicts the distinct redox behavior from the FTIR spectra of UTD in comparison to the 8-ZnTD and 10-ZnTD samples. In this analysis, the anodic and cathodic peak currents (Ipa and Ipc) were extracted through software-based peak analysis. The values obtained through software integration, are as follows: Ipa (UTD) ≈ + 1.8 μA, Ipa (8-ZnTD) ≈ + 5.5 μA, Ipa (10-ZnTD) ≈ + 6.8 μA, along with the corresponding Ipc (UTD) ≈ − 7.0 μA, Ipc (8-ZnTD) ≈ − 4.4 μA, and Ipc (10-ZnTD) ≈ − 6.8 μA. These values were determined by identifying the local maxima and minima in the forward and reverse scans, respectively. This method is consistent with established electrochemical protocols, in which peak currents are identified as the maximum absolute current values in the corresponding scan direction [38]. The Ipa is the indication of the oxidation process of the primary redox-active species (anthocyanin cations) present in acidic anthocyanin solutions. In this regard, the notable increase in Ipa with $ZnSO_4$ treatment indicates an enhancement in dye stabilization and a significant improvement in electron transfer kinetics. Generally, Zn^{2+} ions form stable chelates with the functional groups of anthocyanins. This stable chelates maintaining the integrity of the flavylium structure and enhancing the coupling between the dye and the electrode. Ghosh et al.[39] reported that metal ion coordination improves redox accessibility and peak current intensity in flavonoid-based systems. Moreover, the Ipc indicates the degree to which electrons are returned to the oxidized dye during the reverse scan. In the UTD sample, the Ipc value is measured at − 7.0 μA, signifying a significant level of back-electron transfer. However, following the treatment with $ZnSO_4$, the Ipc decreases to − 4.4 μA in the 0.8-Zn sample and − 6.8 μA in the 10-ZnTD sample. This downward trend which represents the most important and fundamental characteristic of Zn^{2+}-induced recombination suppression.

By facilitating surface trap passivation on TiO_2 with Zn^{2+}, the susceptibility of the oxidized dye structure to recombination is improved. The surface trap states represent the entities that increase the probability of electron recombination with the oxidized dye or electrolyte species, thereby leading to a reduction in Ipc. Rajpar et al. [40] indicate that the Zn^{2+}-modified TiO_2 structures exhibit reduced recombination rates and improved charge separation, even in the absence of supplementary blocking layers.

The indicator for mitigation of recombination can be witnessed through the suppression of Ipc of an electrochemical analysis. Sulaiman et al. [41] reported that ZnO-based blocking layers decreased Ipc and

improved charge retention in DSSCs. Therefore, the behavior of the Ipc witnessed in this study can be closely linking to the effect of Zn^{2+}'s capacity to adjust surface energetics and reduce electron leakage. It is reported that the presence of Zn at the interfaces contributes to a reduction in recombination at the semiconductor junctions, leading to lower Ipc values and improved device performance [42]

Thus, the lower Ipc values observed in Zn-treated dye solutions indicate that Zn^{2+} had effectively suppresses back-electron flow and effectively mitigating recombination. With regards to the 8-ZnTD sample, where the equilibrium between dye stabilization and surface passivation seems to be at its most effective. However, the 10-ZnTD sample, although demonstrating a lower Ipc in comparison to UTD, may indicate partial recombination as a result of over-chelation or ionic crowding.

3.6 Incidence Photon-Current Efficiency, IPCE

Figure 6 depicts the IPCE spectra of various ZnTD DSSC cells (6-ZnTD-Cell, 8-ZnTD-Cell, and 10-ZnTD-Cell) in comparison to the UTD-Cell. The untreated sample displays a narrow and shallow IPCE peak centered between 430 and 440 nm, with a maximum efficiency of less than 0.1%. The restricted spectral response is closely associated with its singular absorption band of the flavylium cation in the visible region of the UV-Vis absorbance profile. It can be clearly seen that the dye exhibits inefficient electron injections and reduced photocurrent generation, which could be attributed to the absence of Zn^{2+} coordination.

Meanwhile, in the case of 8-ZnTD-Cell, a significantly enhanced IPCE peak is observed in the region of 450 to 700 nm, reaching into the near-infrared region. The expanded and intensified spectral response of the IPCE is closely associated the corresponding UV-Vis absorbance characteristics of Zn^{2+}-chelated anthocyanin. This behavior is mainly attributed to the increased molar absorptivity and red-shifted absorption bands as a result of metal–ligand complexation. Roy et al. [43] reported the similar behavior between UV-Vis absorbance and IPCE when investigating the coordination of metal ions in natural dye-sensitized systems.

Noteworthy, the IPCE spectra of the 10-ZnTD cell is lower than the 8-ZnTD cell, despite its highest UV-absorbance compared to both samples. This establishes that the enhanced photocurrent generation is not necessarily the outcome of higher light absorption capability, and its disparity may stem from various interfacial and kinetic factors. For instance, excess $ZnSO_4$ may enhance dye-metal complexation, hence altering the excited-state energetics of anthocyanin. Excess alteration of dye-metal complexation may reduce its electron injection efficiency into TiO_2 [35]. The increased in ionic strength of $ZnSO_4$ may compress the electrical double layer, hence accelerate the recombination of injected electrons and consequently diminish the charge collection efficiency [48]. Additionally, in the condition of higher salt concentrations being added to the solution, dye molecules may aggregate and cause in non-productive exciton pathways [49]. These results highlight the importance of tuning an optimal amount of $ZnSO_4$ loading to maximize the cell.

3.7 Power Conversion Efficiency, PCE

Figure 7 shows the photovoltaic characteristics plot of the UTD-cell in comparison to all types of ZnTD-cells investigated in this study. Meanwhile, Table 2 tabulates the corresponding photovoltaic properties for each of the cells. The 8-ZnTD-cell exhibits the highest overall power conversion efficiency, PCE when compared to the UTD-cell and even to 10-ZnTD-cell. Noteworthy that, further adding the amount of $ZnSO_4$ have caused the fill factor, FF of the 10-ZnTD cell goes down from 0.41 (in the 8-ZnTD) to 0.30. This has led to a decline in the overall efficiency of the cell after it had already reached the maximum PCE with the 8-ZnTD-cell. This situation could be attributed to the increase of series resistance (Rs) due to congestion and ionic crowding at the interface when Zn^{2+} concentrations are too high. Furthermore, the excess Zn^{2+} ions can disrupt the electrons transfer between the dye and TiO_2, and impeding the charge extraction in the system. Nissfolk et al. [44] suggested that elevated Rs in ZnO-based DSSCs may result from excessive surface modifiers or insufficient contact between the photoanode and electrolyte, both of which flattened I–V curve and reduced FF. Additionally, high levels of Zn^{2+} loading may weaken the coordination environment at the interface, which can lead to more recombination. Moderate amounts of Zn^{2+} effectively passivate surface traps on TiO_2 and make dye anchoring more stable. Unfortunately, excessive Zn^{2+} causes the coordination geometry saturated or distorted, which may create new recombination pathways. Wang et al. [45] reported that higher dosage of metal ions can make interfacial selectivity worse, which makes electrons flow back from TiO_2 to the oxidized dye or electrolyte. The recombination process lowers FF and slightly lowers Voc, as seen in the 10-ZnTD sample.

Table 2
Photovoltaic properties of ZnTD cells in comparison to UTD cell.

Cell's Type	J_{SC} (mA/cm^2)	V_{OC}	FF	□ %
UTD	0.52	0.46	0.44	0.11
2-ZnTD	0.88	0.50	0.43	0.19
6-ZnTD	1.36	0.51	0.44	0.31
8-ZnTD	1.74	0.53	0.41	0.38
10-ZnTD	2.27	0.52	0.30	0.35

Moreover, an additional contributing aspect that makes higher concentration of Zn^{2+} detrimental is the formation of multilayer assemblies or agglomerate on the TiO_2 surfaces. This may disrupt uniform electron injections and resulting in heightened interfacial disorder. Fabregat-Santiago et al. [46] established a relationship between dye aggregation and a reduction in FF due to excess metal ion treatment. They also emphasized that such conditions could cause escalation in recombination losses. At the same time, dye aggregation generates areas with diminished conductivity and obstructing charge transport.

In other words, Zn^{2+} overloading alters the local ionic environment and thus affecting the accessibility of the redox pair to the dye–TiO_2 interface. Again, the presence of extensive Zn^{2+} coverage hinders electrolyte diffusion, hence slowing charge regeneration and increasing the likelihood of recombination. Kumar et al. [47] highlights that ionic diffusion barriers in DSSCs significantly influence FF, despite the Jsc being sustained at an elevated level.

Conclusion

This study demonstrates the mechanistic role of $ZnSO_4$ treatment in improving the performance of anthocyanin-sensitized TiO_2-based DSSCs. Utilizing a thorough array of characterizations such as FESEM, UV–Vis spectroscopy, FTIR, pH analysis, CV, IPCE, and J–V measurements, we revealed that Zn^{2+} coordination and protonation markedly enhance the structural, optical, and electrochemical properties of the dye–semiconductor interface.

In this study, Zn^{2+} ions establish stable chelation complexes with anthocyanin, thereby enhancing the spectral integrity of the most photoactive form of the dye called as flavylium cation. The UV–Vis analysis confirms the improvement of molar absorptivity and expansion in the absorption spectrum. Additionally, the $ZnSO_4$ treatment results in a regulated protonation of the dye solution, with the pH decreasing from 3.76 in the UTD to 2.61 in the 10-ZnTD sample. The flavylium cations are preserved from excessive protonation or dye degradation when subjected to this mild protonantion approach which helps maintain spectral integrity and anchoring efficiency.

The FESEM morphological analysis indicates that Zn^{2+} facilitates the formation of a cohesive network of mixed-size nanoparticles between Zn-TiO. This circumstance reduces interfacial voids by improving dye penetration and adsorption. In the meantime, the ZnTD's CV analysis showed that the charge transfer kinetics and redox reversibility had improved, hence diminishing internal resistance. In the IV analysis, the Voc of Zn-TD DSSCs were enhanced due to the improved energy level alignment and decreased recombination. Again, IPCE also confirms that Zn^{2+} coordination improves photon-to-current conversion throughout the visible spectrum, especially in the 8-ZnTD and 10-ZnTD formulations. In conclusion, the application of $ZnSO_4$ as the metal-salt treatment agent presents an effective approach to enhance dye chemistry, interfacial structure, and electron injection pathways, which contributed to the highest PCE of the 8-ZnTD-cell in DSSCs applications.

Declarations

CRediT authorship contribution statement

A.M. Shahrul: Data curation, Formal analysis, Writing – review & editing, Investigation. **N.D.M. Sin**: Formal analysis, Resources, Software, **M.H. Mamat**: Supervision, Conceptualization, Validation. **R. Radzali**: Data curation, Validation, Methodology. **ZHC Soh**: Software, Validation. **Mj. Jalil**: Data curation, Validation, Project administration. **WI Nawawi**: Data curation, Investigation, Validation. **A. Supriyanto**:

Administration, Conceptualization, Resources. **R. Suryana**: Validation, Formal analysis. **M.H. Abdullah**: Conceptualization, Investigation, Methodology, Project administration, Formal analysis, Supervision, Validation, Writing – review & editing.

Acknowledgement

The author(s) acknowledges UiTM Malaysia, and UNS, Indonesia. This research was fully funded by Schema Research of International Collaboration Grant with Number: 369/UN27.22/PT.01.03/2025 Universitas Sebelas Maret, Indonesia.

References

1. H. E. Khoo, K. N. Azlan, A. Ismail, and M. S. Abas, “Anthocyanidins and anthocyanins: Colored pigments as food, pharmaceutical ingredients, and the role of pH,” J. Funct. Foods, vol. 30, pp. 208–222, 2017.
2. S. Rahman et al., “Research on dye sensitized solar cells: Recent advancement toward the various constituents of dye sensitized solar cells for efficiency enhancement and future prospects,” RSC Adv., vol. 13, pp. 19508–19529, 2023.
3. R. Kumar, S. Singh, and A. Sharma, “Metal ion tuning in natural dye-sensitized solar cells: Interfacial dynamics and performance limits,” J. Mater. Chem. C, vol. 11, no. 2, pp. 456–468, 2023.
4. M. A. Hossain, M. S. Islam, and M. M. Rahman, “Performance enhancement of natural dye-sensitized solar cells using metal ion co-sensitization,” Sol. Energy, vol. 245, pp. 1–10, 2022.
5. A. A. Adeyemi and O. O. Ajayi, “The anthocyanin–metal interactions: An overview,” J. Chem. Soc. Nigeria, vol. 47, no. 1, pp. 1–14, 2023.
6. Y. Liu, J. Zhang, and H. Wang, “Chelation-driven enhancement of anthocyanin-sensitized DSSCs using Zn^{2+} and Cu^{2+} co-doping strategies,” Sol. Energy Mater. Sol. Cells, vol. 240, p. 111728, 2022.
7. M. S. Islam, M. A. Hossain, and S. M. Rahman, “Effect of pH and metal ion complexation on the stability and performance of anthocyanin dyes in DSSCs,” J. Photochem. Photobiol. A: Chem., vol. 429, p. 113945, 2023.
8. Y. Zhang et al., “Spectroscopic analysis of TiO_2 nanostructures for solar applications,” J. Mater. Chem. A, vol. 8, no. 12, pp. 6201–6210, 2020.
9. L. Chen et al., “Role of Zn^{2+} in dye–TiO_2 interfacial stabilization,” ACS Appl. Mater. Interfaces, vol. 14, no. 3, pp. 2345–2354, 2022.
10. V. Kumar et al., “Zn^{2+} surface modification of TiO_2: FTIR and photovoltaic implications,” J. Photochem. Photobiol. A: Chem., vol. 402, p. 112812, 2020.
11. S. Ramesh et al., “FTIR evidence of metal–oxide coordination in DSSC interfaces,” J. Mol. Struct., vol. 1171, pp. 45–52, 2018.

12. H. Li et al., “FTIR and XPS study of metal–TiO_2 interactions in hybrid systems,” Surf. Sci. Rep., vol. 74, no. 3, pp. 89–104, 2019.
13. J. Nissfolk et al., “Identification of factors giving low fill factor in ZnO-based dye-sensitized solar cells,” J. Phys. Chem. C, vol. 113, no. 24, pp. 10936–10941, 2009.
14. M. Fabregat-Santiago et al., “Dye aggregation and recombination losses in DSSCs,” J. Electrochem. Soc., vol. 156, no. 1, pp. H1–H7, 2009.
15. A. A. Khan et al., “Magnesium sulfate as a potential dye additive for chlorophyll-based organic sensitiser of the dye-sensitised solar cell (DSSC),” Spectrochim. Acta A: Mol. Biomol. Spectrosc., vol. 274, p. 121140, 2022.
16. M. H. Abdullah, M. S. Adilah, E. Noorsal, C. A. C. Azurahanim, M. H. Mamat, M. K. Ahmad, and M. Rusop, “Synergistic effect of complementary organic dye co-sensitizers for potential panchromatic light-harvesting of dye-sensitized solar cells,” Opt. Mater., vol. 133, p. 113016, 2022.
17. Y. Zhang et al., “Surface modification of TiO_2 with Zn^{2+} ions for enhanced dye loading and photovoltaic performance,” Appl. Surf. Sci., vol. 546, p. 149103, 2021.
18. H. Li et al., “Morphological and interfacial analysis of dye-sensitized TiO_2 photoelectrodes: Effect of metal-free versus metal-complex dyes,” J. Photochem. Photobiol. A: Chem., vol. 400, p. 112609, 2020.
19. S. Ghosh et al., “Metal ion doping in TiO_2: Structural and surface chemistry implications for solar energy conversion,” J. Phys. Chem. C, vol. 127, no. 12, pp. 6543–6552, 2023.
20. L. Velpuri et al., “Photovoltaic performance of TiO_2 and ZnO nanostructures in anthocyanin dye-sensitized solar cells,” Clean Energy, vol. 8, no. 5, pp. 144–156, 2024.
21. Pawar P.S. et al., “TiO_2/ZnO nanocomposites with a metal-free dye and a polymer gel electrolyte: optimizing photovoltaic efficiency,” Energy Advances, vol. 4, 2025.
22. Yildiz A. et al., “Review on TiO_2 nanotubes in dye-sensitized solar cells: electrochemical performance and recombination control,” J. Solid State Electrochem., vol. 29, 2024.
23. Devi R. et al., “Zn^{2+}-modified TiO_2 interfaces for enhanced dye anchoring and surface passivation,” Mater. Chem. Phys., vol. 295, pp. 126–134, 2023.
24. Roy, S., et al. (2020). Anthocyanin food colorant and its application in pH-responsive color change indicator films. Critical Reviews in Food Science and Nutrition, PDF
25. Rhim, J.-W., et al. (2020). Anthocyanin-based pH indicators for smart packaging. Food Hydrocolloids, 105, 105–112.
26. Khoo, H.E., et al. (2017). Anthocyanidins and anthocyanins: Colored pigments as food, pharmaceutical ingredients, and the role of pH. Journal of Functional Foods, 30, 208–222.
27. Zhang, Y., et al. (2016). Spectral tuning of anthocyanin dyes via metal ion coordination. Dyes and Pigments, 132, 142–150.
28. Kong, J., et al. (2014). Metal–anthocyanin complexes and their role in DSSC performance. Journal of Photochemistry and Photobiology A: Chemistry, 280, 1–8.

29. Gulcin, İ., & Alwasel, S. H. (2022). Metal ions, metal chelators and metal chelating assay as antioxidant method. Processes, 10(1), 132.
30. Adeagbo, A. I., Azeez, A. A., Ogunmola, O. O., Sodamade, A., & Larayetan, R. A. (2024). The anthocyanin metal interactions: An overview. Journal of the Chemical Society of Nigeria, 49(5), 669–682.
31. Hao, S., et al. (2006). Metal ion effects on the performance of natural dye-sensitized solar cells. Solar Energy, 80(2), 209–214
32. F. Mollaamin and M. Monajjemi, “Dye-sensitized solar cells: A theoretical study on natural pigments as sensitizers,” J. Mol. Struct.
33. A. S. Al–Saadi, H. A. Al–Saadi, and M. A. Al–Saadi, “Dye–sensitized solar cells: Meta–analysis of effect sensitizer–type on photovoltaic performance,” Heliyon, vol. 10, no. 2, p. e17123, 2024. doi: 10.1016/j.heliyon.2024.e17123.
34. J. M. Custodio–Mendoza, A. Hernández–Martínez, and R. Gómez, “Recent progress in natural dye–sensitized solar cells: Stability, interfacial engineering, and performance optimization,” Sol. Energy, vol. 272, pp. 1123–1138, 2024
35. R. M. Silverstein, F. X. Webster, D. J. Kiemle, and D. L. Bryce, Spectrometric Identification of Organic Compounds, 8th ed. Hoboken, NJ, USA: Wiley, 2014.
36. A. M. El–Naggar, “FTIR analysis of dye–semiconductor interactions in DSSCs,” J. Mol. Struct., vol. 1205, pp. 127–134, 2020.
37. Ramesh, S. et al. (2018). FTIR evidence of metal–oxide coordination in DSSC interfaces. Journal of Molecular Structure.
38. Johns Hopkins University, “Cyclic Voltammetry: Principles and Interpretation,” Department of Chemistry, PDF
39. Ghosh S. et al., “Metal ion doping in TiO_2: structural and surface chemistry implications for solar energy conversion,” J. Phys. Chem. C, vol. 127, no. 12, pp. 6543–6552, 2023.
40. Rajpar A.H. et al., “Fabrication and Enhanced Performance Evaluation of TiO_2@Zn/Al-LDH for DSSC Application,” Nanomaterials, vol. 14, no. 11, 2024.
41. Sulaiman N. et al., “Impact of blocking layers based on TiO_2 and ZnO prepared via direct deposition on DSSC recombination,” Scientific Reports, vol. 14, 2024.
42. Asemi M. et. al,. “Minimizing the charge recombination rate at the FTO/Zn_2SnO_4 interface,” Journal of Materials Science, vol. 53, pp. 7551–7561, 2018.
43. Roy, S., et al. (2020). Anthocyanin food colorant and its application in pH-responsive color change indicator films. Critical Reviews in Food Science and Nutrition.
44. Nissfolk, J. et al. (2009). Identification of factors giving low fill factor in ZnO-based dye-sensitized solar cells. Journal of Physical Chemistry C.
45. Wang, J. et al. (2021). Zn-modified TiO_2 interfaces for enhanced dye anchoring. Applied Surface Science.

46. M. Fabregat-Santiago et al., “Dye aggregation and recombination losses in DSSCs,” J. Electrochem. Soc., vol. 156, no. 1, pp. H1–H7, 2009.
47. Kumar, V. et al. (2020). Zn^{2+} surface modification of TiO_2: FTIR and photovoltaic implications. Journal of Photochemistry and Photobiology A.
48. Magnesium sulfate as a potential dye additive for chlorophyll-based organic sensitiser of the dye-sensitised solar cell (DSSC)
49. Shahrul, A. M., Abdullah, M. H., Adilah, M. S., Hadis, N. S. M., Rashid, A. N. A., Ibrahim, M. N., … Rusop, M. (2022). Coactive impact of a novel multifunctional alum co-adsorbent for dye-sensitized solar cells DSSC. Materials Letters, 317, 132088.

Figures

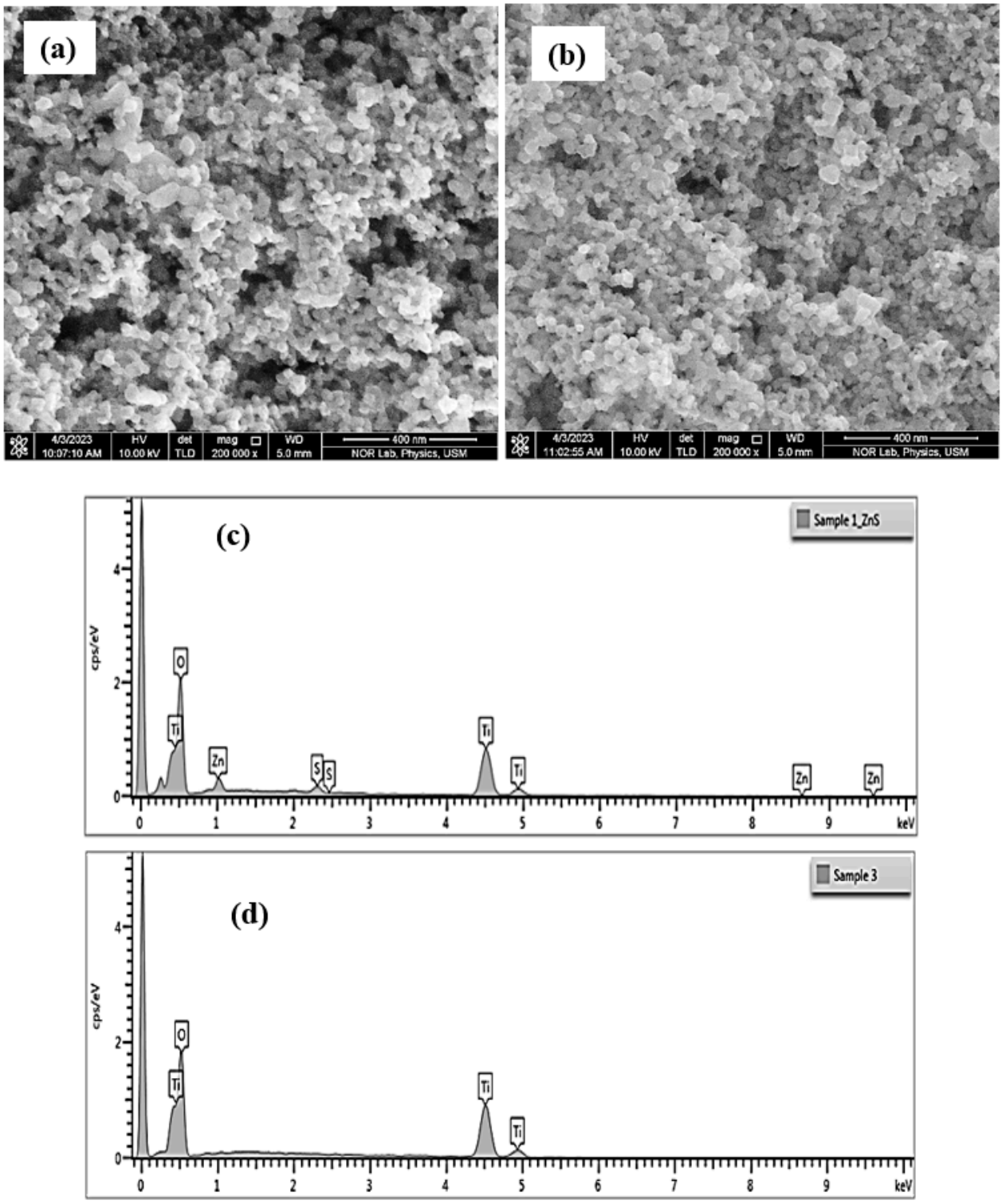


Figure 1

Surface morphology image of TiO_2 photoelectrodes, (a) immersed in $ZnSO_4$-treated anthocyanin, (8-ZnTD), (b) immersed with unmodified anthocyanin (UTD) (c) EDX pattern for TiO_2 immersed in $ZnSO_4$-treated anthocyanin, (d) EDX analysis of the TiO_2 photoelectrode in UTD.

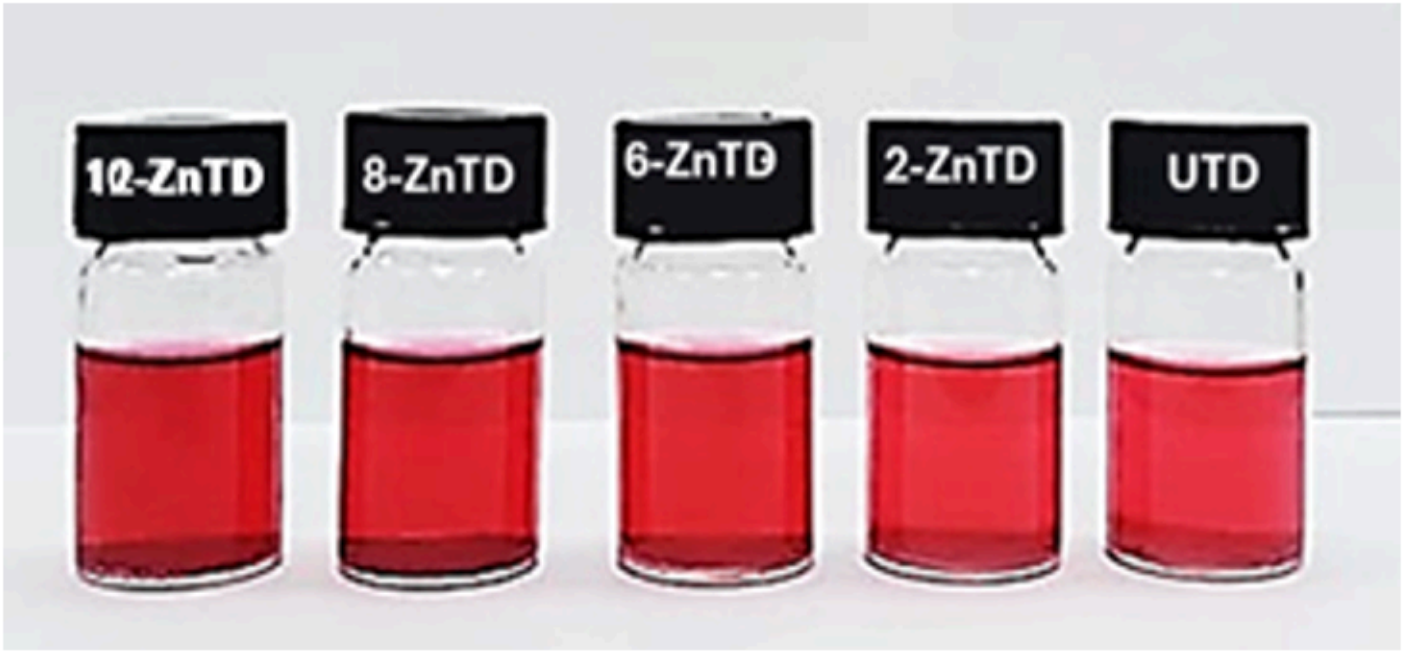


Figure 2

Progressive colour change in methanolic anthocyanin solutions upon the addition of $ZnSO_4$ to ZnTD in comparison to UTD

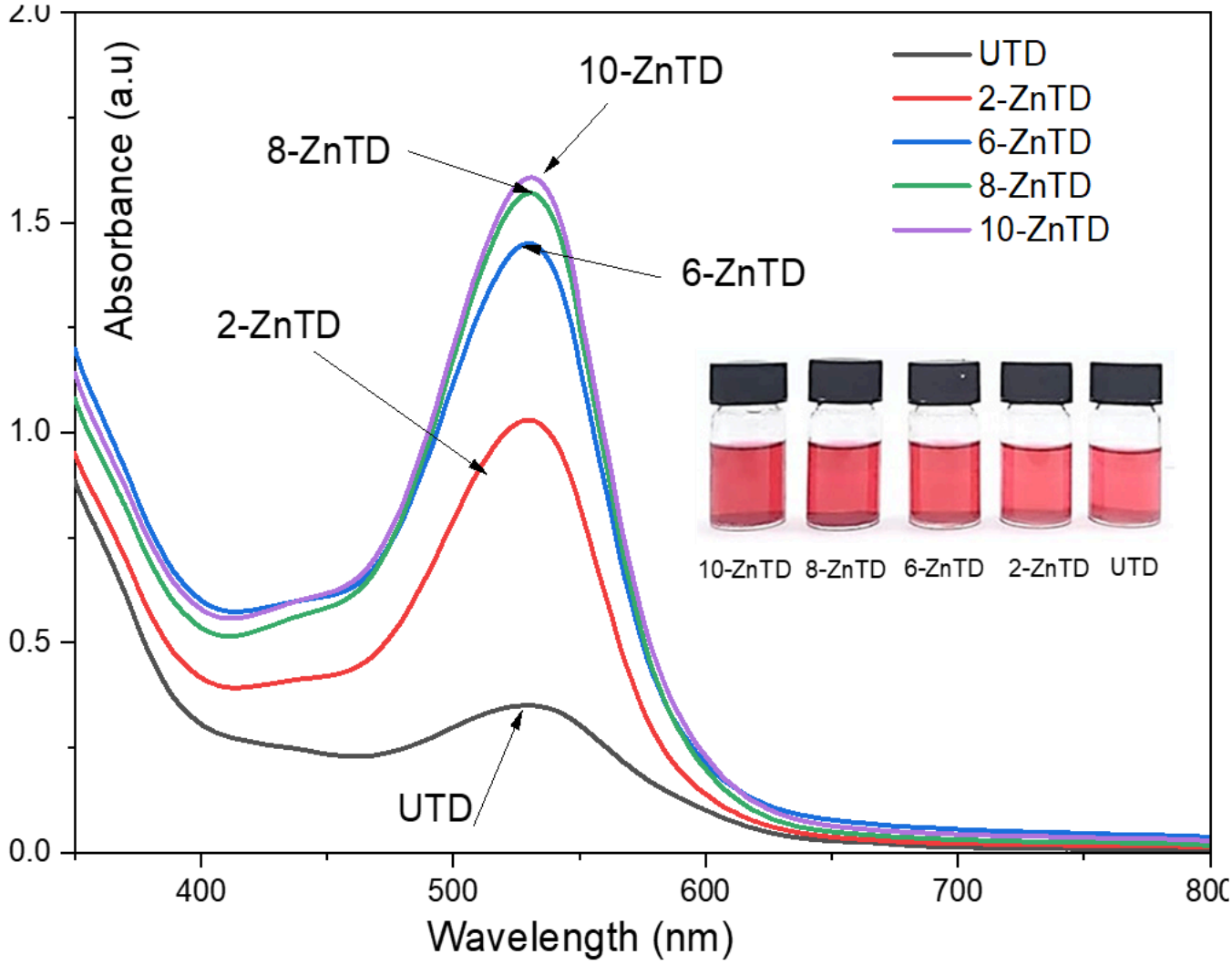


Figure 3

UV- Vis absorbance spectra of UTD in comparison to all ZnTD dye solution at different weight percentage.

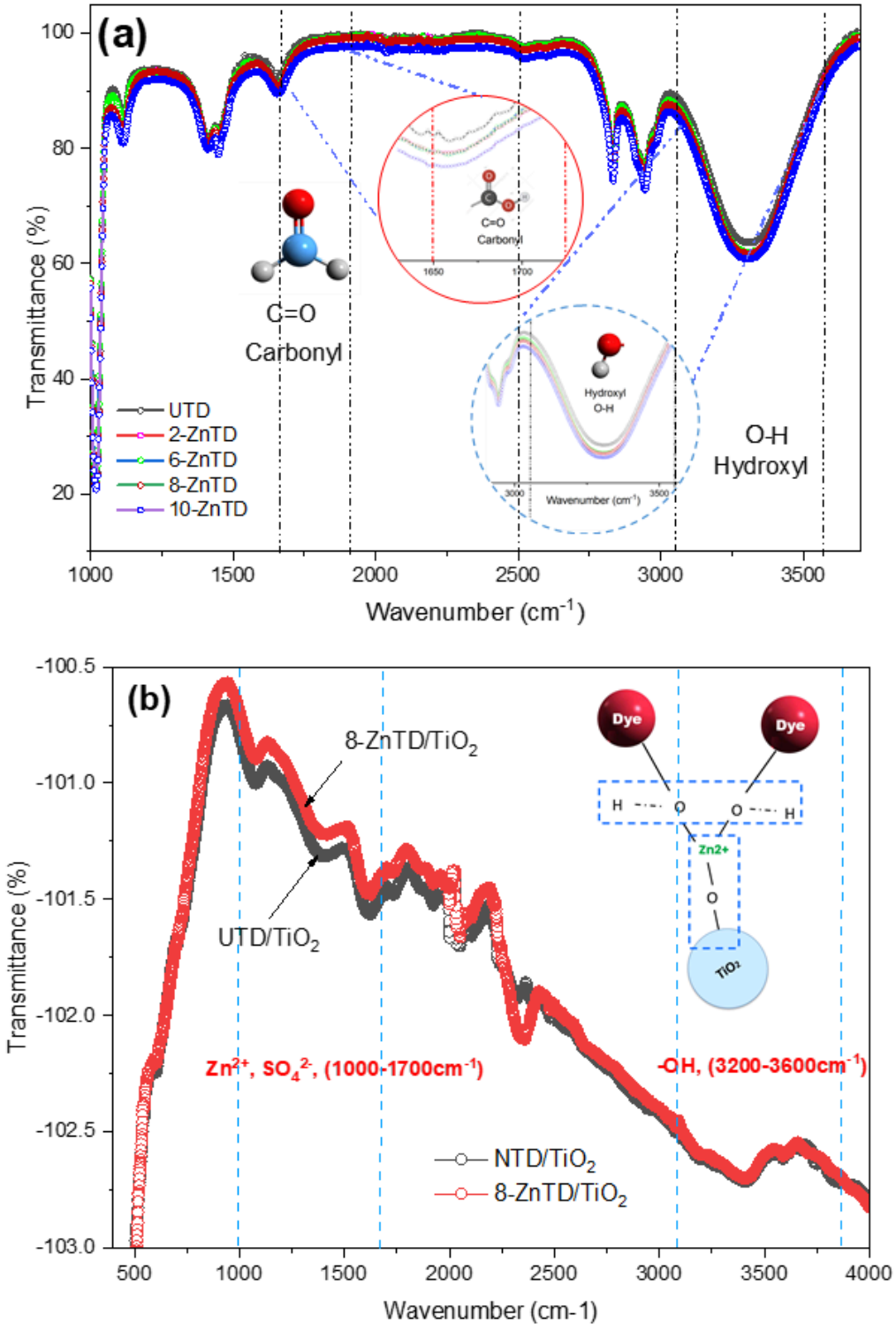


Figure 4

FTIR spectra of UTD in comparison to ZnTD (a) solution based, (b) TiO_2 nanoparticles of UTD/TiO_2 versus 8-ZnTD/TiO_2 immersed in respective dyes,

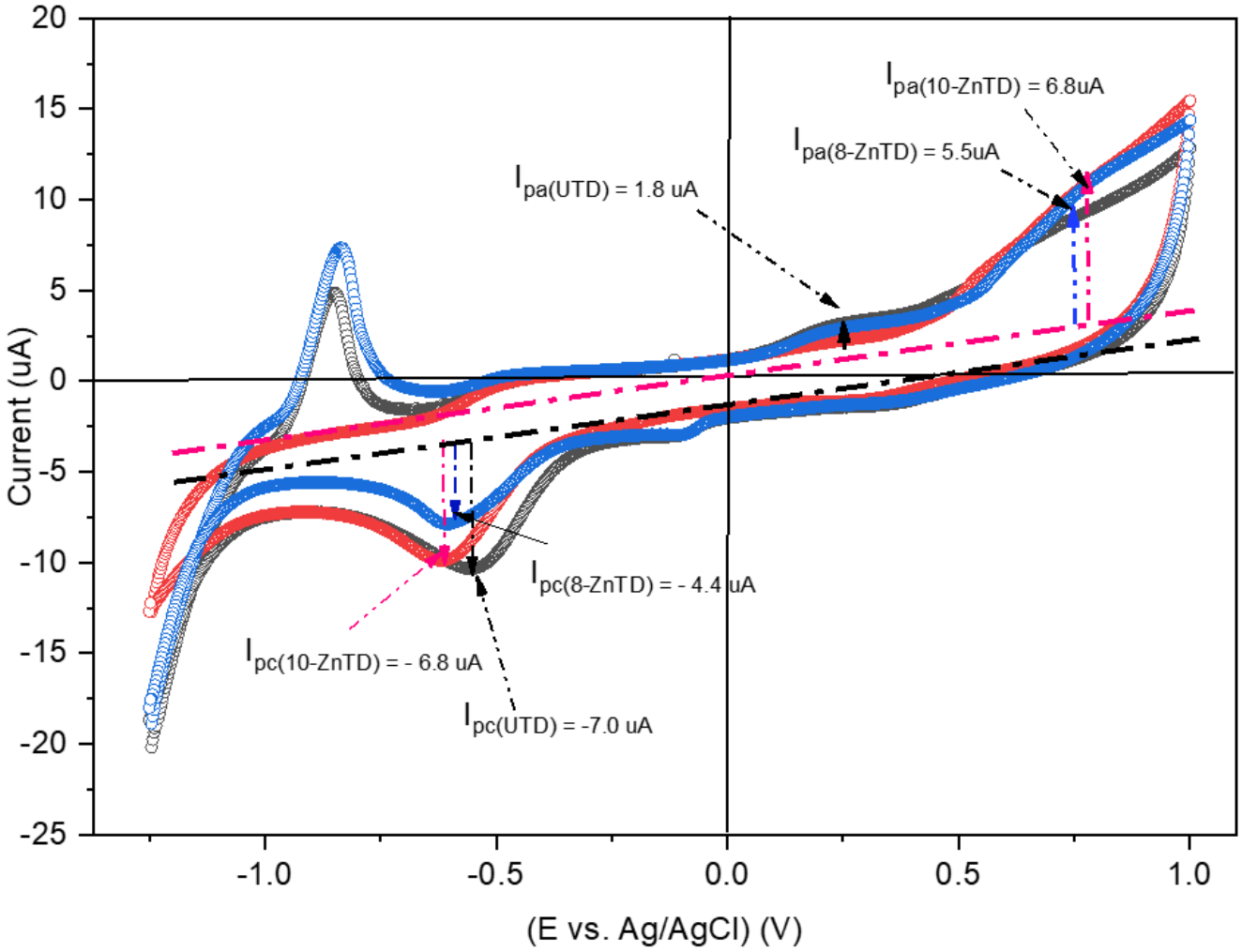


Figure 5

Cyclic Voltammetry spectra of UTD in comparison to 8-ZnTD and 10-ZnTD anthocyanin dye solutions.

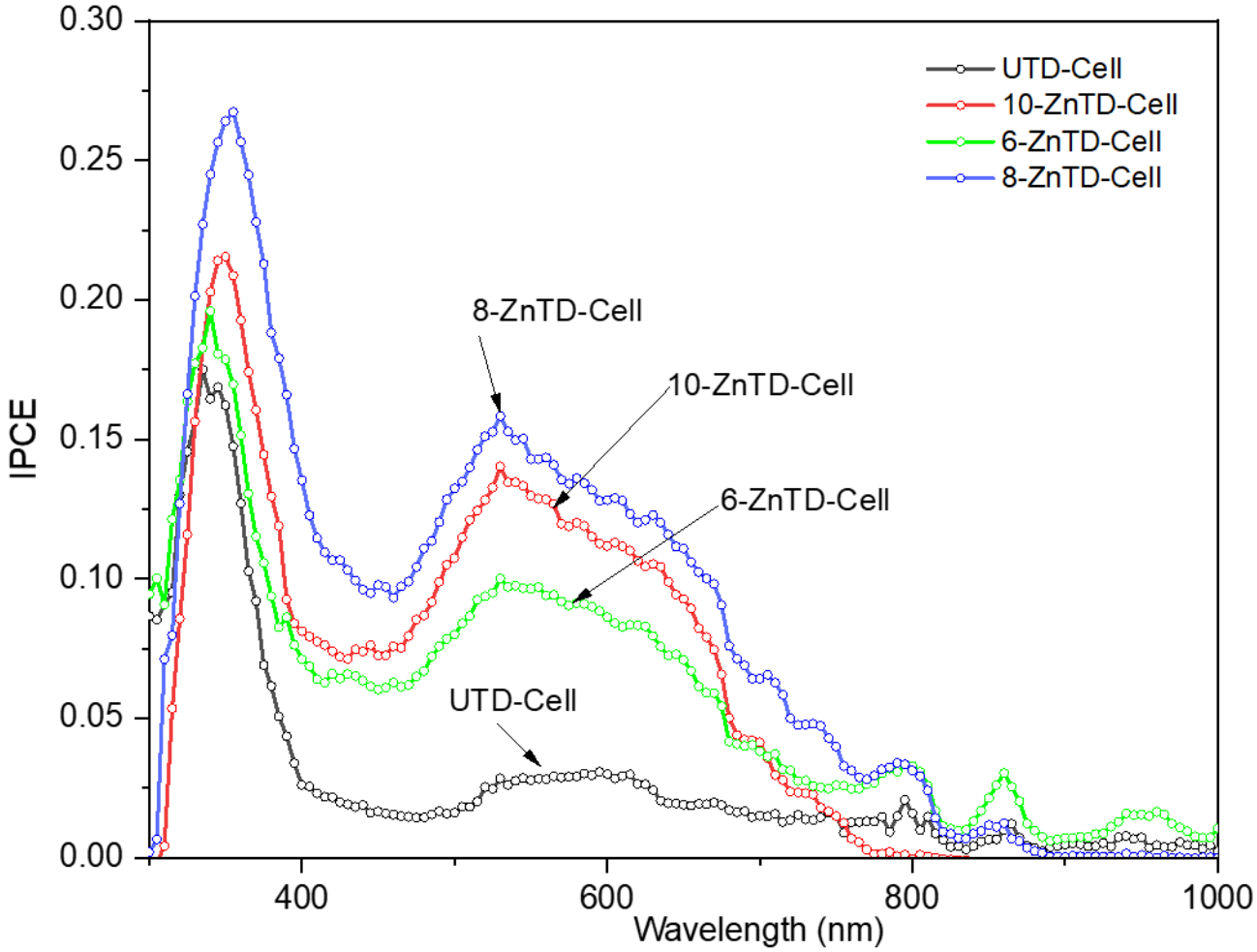


Figure 6

Cyclic Voltammetry spectra of UTD in comparison to 6-ZnTD, 8-ZnTD and 10-ZnTD DSSC cells.

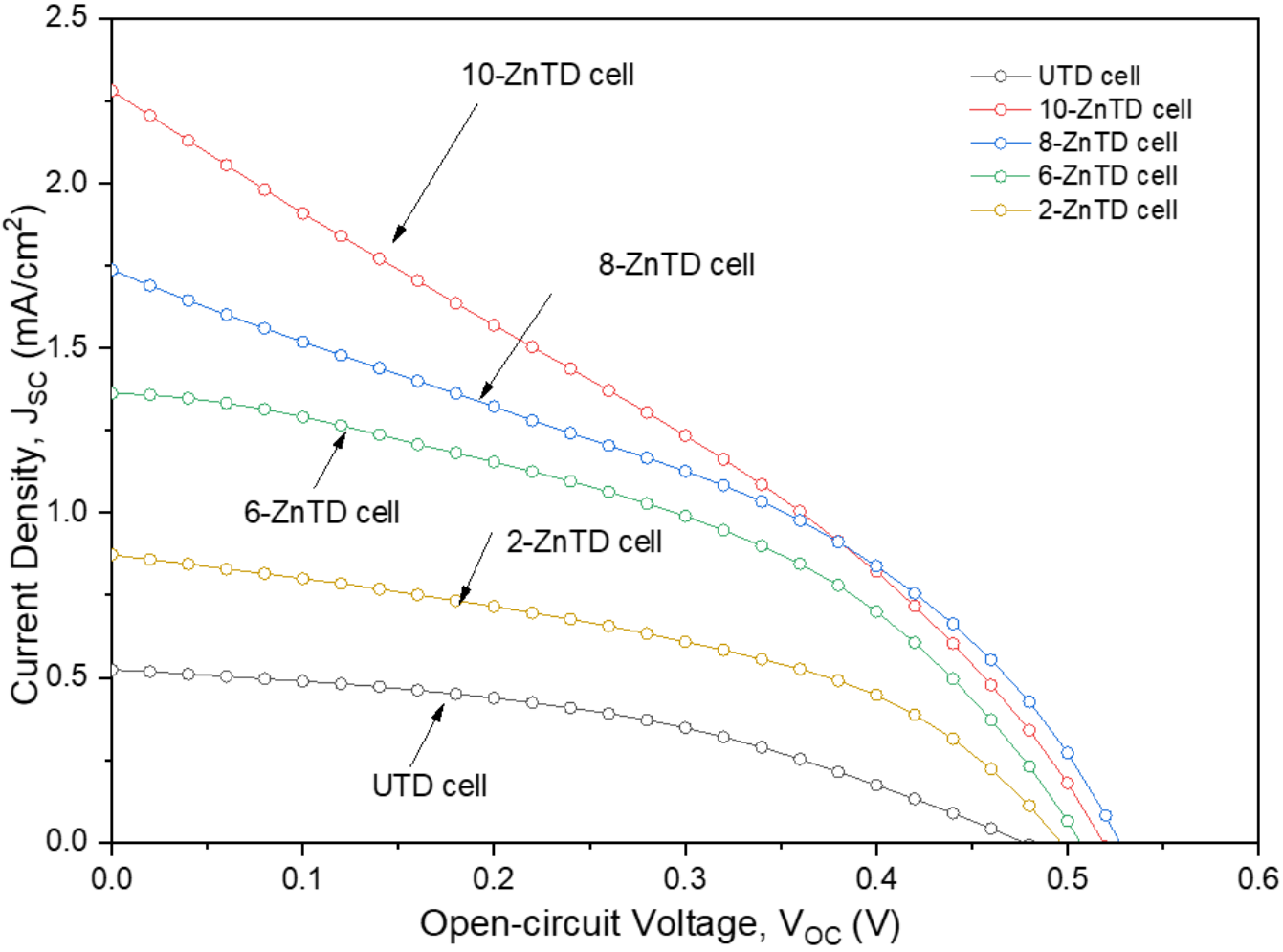


Figure 7

Photovoltaic characteristics of various ZnTD cells versus the UTD cells.